Journal of Hydraulic Research Vol. 45, No. 4 (2007), pp. 519–528

A Boussinesq-type model for flow over trapezoidal profile weirs

Un modèle de type Boussinesq pour les déversoirs trapézoïdaux de profil d'excédent d'écoulement

YEBEGAESHET T. ZERIHUN, *Department of Water, Land and Biodiversity Conservation, GPO Box 2834, Adelaide, SA 5001, Australia. Tel.: +61 8 8463 6986; fax: +61 8 8463 6999; e-mail: Zerihun.Yebegaeshet@saugov.sa.gov.au*

JOHN D. FENTON, *Institut für Hydromechanick, Universität Karlsruhe (TH), D-76131 Karlsruhe, Germany. Tel.: +49(0) 721 608 7245; fax: +49(0) 721 608 2202; e-mail: fenton@ifh.uka.de*

ABSTRACT
Computational flow models that are developed based on the depth-averaged Saint–Venant equations cannot be used to simulate flow over short- and broad-crested trapezoidal profile weirs. In the derivation of the Saint–Venant equations, uniform velocity and hydrostatic pressure distributions have been assumed. These assumptions restrict the application of the equations to flow situations with insignificant curvature of streamlines. In this study a Boussinesq-type momentum equation, which allows for curvature of the free surface and a non-hydrostatic pressure distribution, along with a simplified equation for weakly curved free surface flow, are investigated for the numerical simulation of steady flow over short- and broad-crested types of these weirs with smooth and rough flow boundaries. The finite difference method is employed to discretize and solve these nonlinear flow equations. Computed and measured results of flow surface and bed pressure profiles for these types of weirs are presented. The Boussinesq-type momentum equation performs satisfactorily for both subcritical and transcritical flow situations, while the simplified equation simulates these flow situations on rough flow boundaries fairly well. The overall prediction results validate the use of the weak curvature approximation.

RÉSUMÉ
Les modèles numériques d'écoulement basés sur les équations de Saint–Venant moyennées en profondeur ne peuvent pas simuler les écoulements sur les déversoirs trapézoïdaux de courte ou de large crête. En effet, pour établir les équations de Saint–Venant, on suppose que la vitesse est uniforme et les pressions hydrostatiques. Ces hypothèses limitent l'application de ces équations aux situations dans lesquelles la courbure des lignes de courant est insignifiante. Dans cette étude une équation des quantités de mouvement de type Boussinesq, qui tient compte de la courbure de la surface libre et d'une distribution non-hydrostatique de pression, ainsi qu'une équation simplifiée pour les écoulements avec surface libre faiblement incurvée, sont étudiées pour simuler numériquement un écoulement permanent sur ces déversoirs de types courte ou large crête avec des frontières d'écoulement lisses ou rugueuses. Ces équations non-linéaires sont résolues par une méthode de discrétisation en différences finies. Des résultats calculés et mesurés des profils de surface libre et de pression de lit pour ces types de déversoirs sont présentés. L'équation des quantités de mouvement de type Boussinesq permet de calculer d'une manière satisfaisante les situations sous-critiques et transcritiques de l'écoulement, alors que l'équation simplifiée simule vraiment bien ces situations d'écoulement sur des frontières rugueuses. Les résultats globaux de prévision valident l'utilisation de l'approximation de faible courbure.

Keywords: Flow simulation, embankment weir, hydrodynamics, Boussinesq equation, rapidly varied flow.

1 Introduction

Numerical and experimental studies of flow over trapezoidal profile weirs have a number of applications especially in the analyses of flow over common types of civil engineering structures. For instance, simulation of flood flows over highway and railway embankments are analogous to the case of flow over short- and broad-crested trapezoidal profile weirs. The free overflow characteristics of these weirs often provide important boundary conditions for the application of large two-dimensional flow models. The significant nature of flow over such types of weirs, especially in the vicinity of flow transition from subcritical to supercritical state, is a strong departure from the hydrostatic distribution of pressure, caused by the curvatures of the streamlines. Most of the existing computational flow models, which are based on the depth-averaged Saint–Venant equations, are inappropriate to simulate this type of flow problem. In the derivation of the Saint–Venant equations, assumptions of uniform velocity and hydrostatic pressure distributions are commonly employed. Consequently, the equations represent the lowest-order in approximation and cannot retain accuracy for flow situations that involve non-hydrostatic pressure and non-uniform velocity distributions (see e.g. Bhallamudi and Chaudhry, 1992; Berger, 1994). The two-dimensional nature of the flow over these weirs requires more accurate methods for exact simulation of the flow situation. In this paper, the Boussinesq-type momentum

Revision received September 14, 2005/Open for discussion until February 29, 2008.

equation models will be employed for the numerical simulation of such type of flow problem.

Studies to understand the basic mechanics of free surface flow with considerable curvature of streamlines date back to the earliest attempt by Boussinesq (1877). Boussinesq (1877) was the first to extend the momentum equation to incorporate implicitly the effect of curvature of the streamlines using the assumption of a linear variation of curvature of streamlines from the bed to the free surface. Recently, Dressler (1978) developed a set of shallow-flow equations for irrotational flow using an orthogonal bed-fitted curvilinear coordinate system. Sivakumaran and Yevjevich (1987) studied the applicability of these equations for free flow over a spillway. They obtained results that are in good agreement with measurements. Even though the equations do describe some phenomena well, the Dressler's method does not permit flow regime to change from subcritical to supercritical state (see e.g. Sivakumaran *et al.*, 1983). Hager and Hutter (1984), Hager (1985) and Matthew (1991) presented Boussinesq-type energy equations based on a potential-flow assumption for modelling two-dimensional flows over curved boundaries. Steffler and Jin (1993) developed the vertically averaged and moment (VAM) equations based on the assumptions of a linear longitudinal velocity distribution, and quadratic pressure and vertical velocity distributions across the depth of flow. The resulting equations are long and complex. Khan and Steffler (1996a,b) successfully applied these equations to the simulation of different curved flow problems.

Fenton (1996) introduced alternative Boussinesq-type momentum equations to model flow with a non-hydrostatic pressure distribution. Compared to other governing equations (for instance, Dressler and VAM equations), the equations are simple to apply in a cartesian coordinate system especially for free surface flow problems with continuous flow boundaries. In this work, the applicability of these equations for steady flow over short- and broad-crested trapezoidal profile weirs will be investigated.

The problem of flow over trapezoidal profile weirs has been extensively studied experimentally. Most of the experimental works were performed to understand the flow characteristics of these weirs as well as the determination of the coefficients of discharge under free and submerged flow conditions (see e.g. Fritz and Hager, 1998; Kindsvater, 1964). However, the global flow characteristics including the bed pressure distribution have not been thoroughly investigated. Besides, no work has so far been reported in the literature (to the writers' knowledge) to simulate flow over these weirs numerically using lower- or higher-order governing equations. From a practical perspective, accurate simulation of the flow profile, particularly the upstream water surface elevation, is important in order to predict the discharge capacity of these weirs under free flow conditions. The current numerical procedure presented in this paper for the solutions of the Boussinesq-type equations provides a convenient method of developing head-discharge relationships for short- and broad-crested trapezoidal profile weirs with smooth and rough beds, thus extending the existing methodology or procedure which is applicable to broad-crested weir only. This issue will be addressed in detail in subsequent publications.

Therefore, the main objectives of this paper are: (i) to model subcritical and transcritical flows over trapezoidal profile weirs using Boussinesq-type equations numerically; (ii) to assess the influence of the curvature of the streamlines on the flow surface and bed pressure profile solutions of the equations; and (iii) to demonstrate the validity of the model by a number of laboratory experiments.

2 Governing equations

It is well known that the pressure distribution in free surface curved flows is non-hydrostatic due to the effect of the vertical acceleration of the flow. In the modelling of Boussinesq-type equations, this effect on the flow behaviour can be accounted for implicitly by including the centrifugal term $\kappa/\cos\theta$, where κ is the curvature and θ is the angle of inclination of the streamline with the horizontal axis. The degree of curvature of the streamlines directly influences the magnitude of the term. For a nearly horizontal flow situation where the curvature and slope of the streamline are insignificant, $\kappa \cong 0$ and $\cos\theta \cong 1$.

Fenton (1996) applied the momentum principle along with the simplifying assumption of a constant centrifugal term at a vertical section to develop the equations. In the derivation of these equations the curvatures of the flow surface, κ_{H}, and the bed, κ_{b}, are approximated by the expressions for flow with weak curvature of streamlines, i.e., $\kappa_{\mathrm{H}} \cong \mathrm{d}^2H/\mathrm{d}x^2 + Z_{\mathrm{b}}^{''}$ and $\kappa_{\mathrm{b}} \cong Z_{\mathrm{b}}^{''}$. For steady flow in a rectangular channel the flow equation reads as

$$\begin{aligned}\beta\frac{q^2}{4}\frac{\mathrm{d}^3H}{\mathrm{d}x^3} &+ \beta\frac{Z_{\mathrm{b}}'q^2}{2H}\frac{\mathrm{d}^2H}{\mathrm{d}x^2}\\ &+ \vartheta\left(\left(gH - \beta\frac{q^2}{H^2}\right)\frac{\mathrm{d}H}{\mathrm{d}x} + gH\left(Z_{\mathrm{b}}' + S_{\mathrm{f}}\right)\right)\\ &+ \omega_0\beta q^2\left(\frac{Z_{\mathrm{b}}'''}{2} + \frac{Z_{\mathrm{b}}'Z_{\mathrm{b}}''}{H}\right) = 0, \end{aligned} \tag{1}$$

in which H is the depth of flow; Z_{b}', Z_{b}'' and Z_{b}''' are the first, second and third derivatives of the bed profile, respectively; S_{f} denotes the friction slope, calculated from the Gauckler–Manning–Strickler equation or smooth boundary resistance law; q is the discharge per unit width; β refers to the Boussinesq coefficient; g is gravitational acceleration; $\vartheta = 1 + Z_{\mathrm{b}}'^2$; and ω_0 is a constant factor to reflect the combined effect of the bed in determining the elevation of the surface and the associated dynamic pressures due to slow moving flow near the bottom of the flow boundary. Fenton (1996) suggested a value of slightly less than 1 for ω_0.

The corresponding pressure equation is given by

$$p = \rho(\eta - z)\left(g + \beta\frac{q^2}{\vartheta H^2}\left(\omega_0 Z_{\mathrm{b}}'' + \frac{1}{2}\frac{\mathrm{d}^2H}{\mathrm{d}x^2}\right)\right), \tag{2}$$

in which ρ is the density of the fluid; η is the mean elevation of the free surface; z is the vertical coordinate of a point in the flow field; p is the pressure. If the curvatures of the streamlines and the bed are neglected, i.e., $\mathrm{d}^2H/\mathrm{d}x^2 = Z_{\mathrm{b}}'' = 0$, Eq. (2) reduces to the hydrostatic pressure equation. The second term on the right-hand side of the equation accounts for dynamic effects; it depends

on the curvatures of the bed and streamlines. Since at a vertical section the variation of the centrifugal term is approximated by the average value of the contribution of the bed and the curved flow surface, the excess pressure above the hydrostatic varies linearly with the depth of flow.

3 Nature of the flow equation

Equation (1) implicitly includes the effect of the vertical acceleration to model two-dimensional flow problems where more vertical details are significant and essential. For the case of weakly curved free surface flow with negligible curvature of streamlines in a constant slope channel, the flow surface and bed curvatures terms vanish to zero. Under this flow condition, the above equation degenerates to the gradually varied flow equation.

The last term of the equation (the second and third derivatives of the bed profile) takes into account the effect of the curvature of the bed profile on the streamline behaviour. In a special case of curved flow in a constant slope channel where $Z_b''' = Z_b'' = 0$, the equation reduces to

$$\beta\frac{q^2}{4}\frac{\mathrm{d}^3H}{\mathrm{d}x^3} + \beta\frac{Z_b' q^2}{2H}\frac{\mathrm{d}^2H}{\mathrm{d}x^2} + \vartheta\left(\left(gH - \beta\frac{q^2}{H^2}\right)\frac{\mathrm{d}H}{\mathrm{d}x} + gH\left(Z_b' + S_f\right)\right) = 0. \quad (3)$$

Equation (3) implies that, in contrast to the Dressler equations, the flow equation separately includes the effects of the curvature of the streamline and the flow boundaries. Furthermore, the equation incorporates wave-like variations of the free surface to simulate short waves on such channel. For weakly curved free surface flow in the vertical plane, the products of the derivatives are very small in relation to the derivatives themselves. Neglecting these terms in Eq. (1) gives

$$\beta\frac{q^2}{4}\frac{\mathrm{d}^3H}{\mathrm{d}x^3} + \left(gH - \beta\frac{q^2}{H^2}\right)\frac{\mathrm{d}H}{\mathrm{d}x} + \omega_0\beta q^2\left(\frac{Z_b'''}{2}\right) + gH\left(Z_b' + S_f\right) = 0. \quad (4)$$

A flow equation similar in structure to this equation was first presented by Boussinesq (1877). This equation and Eq. (1) will be referred to hereafter as the weakly curved flow (WCF) equation and the Boussinesq-type momentum (BTM) equation, respectively. Both equations will be used in this study to simulate free surface flow over trapezoidal profile weirs with smooth transition curves introduced at the four corners of the profile for the purpose of integrating the equations continuously at these points. The solutions of these two equations will be compared to examine the influence of the degree of curvature of the flow surface on the solutions of the equations. For the WCF equation, the corresponding pressure equation can be obtained by setting $\vartheta = 1$ in Eq. (2).

4 Problem formulation and boundary conditions

The computational domain for the numerical solution of the weir flow problem is shown in Fig. 1. In this figure, AB is the inflow section, CD is the outflow section, MUVN is the trapezoidal profile weir and AC is the free surface of the flow. The inflow and outflow sections of the computational domain are located in a region where the flow is nearly uniform. This quasi-uniform flow condition before the inflow and after the outflow sections of the solution domain simplifies the evaluation of the boundary values at these sections using the gradually varied flow equation. Thus, for a given depth at the inflow section the slope of the water surface, S_H, can be computed from the gradually varied flow equation:

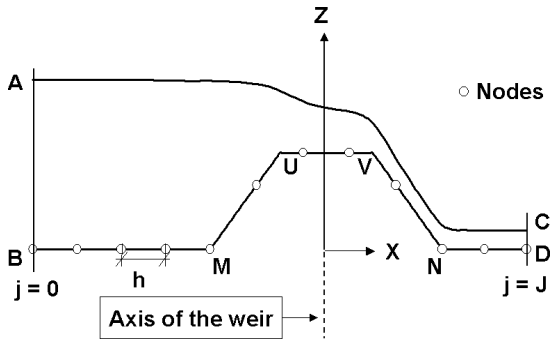

Figure 1 Computational domain for flow over a weir.

$$S_H = \frac{\mathrm{d}H}{\mathrm{d}x} = \frac{S_0 - S_f}{1 - \beta Fr^2}, \quad (5)$$

in which Fr is the Froude number; and S_0 is the bed slope. For the given flow depths, AB and CD, at the inflow and outflow sections, respectively, and discharge at the inflow section, it is required to determine the flow surface profile, AC, and the bed pressures along the centreline of the trapezoidal profile weir. For this purpose the computational domain which is bounded by the free surface of the flow, inflow and outflow sections, and the solid flow boundary is discretized into equal size steps in x as shown in Fig. 1.

5 Numerical model and solution procedure

Analytical solutions are not feasible for the above flow equations due to the presence of strong nonlinear terms. Therefore, a numerical approach based on finite difference approximations is used here for their solutions. This formulation is simple to code and extensively used to solve linear or nonlinear differential equations. For the purpose of discretization, Eqs (1) and (4) can be represented by a simple general equation as

$$\frac{\mathrm{d}^3H}{\mathrm{d}x^3} + \xi_0\frac{\mathrm{d}^2H}{\mathrm{d}x^2} + \xi_1\frac{\mathrm{d}H}{\mathrm{d}x} + \xi_2 = 0, \quad (6)$$

where ξ_0, ξ_1 and ξ_2 are the nonlinear coefficients associated with the equation and the corresponding expressions can be obtained by comparing this equation with the respective flow equations. Both governing equations, Eqs (1) and (4), are third-order differential equations which need to employ third- or higher-order accurate methods to solve the equations numerically. This is necessary in order to reduce the truncation errors introduced in the formulation due to the finite difference approximation

of the derivative terms of the equations (Abbott, 1979). Therefore, four-point finite difference approximations are employed here to replace the derivative terms in the third-order flow equations.

The upwind finite difference approximations (Bickley, 1941) for derivatives at node j are

$$\left(\frac{\mathrm{d}^3H}{\mathrm{d}x^3}\right)_j = \frac{1}{h^3}\left(-H_{j-2} + 3H_{j-1} - 3H_j + H_{j+1}\right), \tag{7}$$

$$\left(\frac{\mathrm{d}^2H}{\mathrm{d}x^2}\right)_j = \frac{1}{3h^2}\left(3H_{j-1} - 6H_j + 3H_{j+1}\right), \tag{8}$$

$$\left(\frac{\mathrm{d}H}{\mathrm{d}x}\right)_j = \frac{1}{6h}\left(H_{j-2} - 6H_{j-1} + 3H_j + 2H_{j+1}\right). \tag{9}$$

Equations (7)–(9) are introduced into Eq. (6) to discretize the derivative terms. After simplifying the resulting expression and assembling similar terms together, the equivalent finite difference equation becomes

$$\begin{aligned} &H_{j-2}\left(-6 + \xi_{1,j}h^2\right) + H_{j-1}\left(18 + 6\xi_{0,j}h - 6\xi_{1,j}h^2\right) \\ &\quad + H_j\left(-18 - 12\xi_{0,j}h + 3\xi_{1,j}h^2\right) \\ &\quad + H_{j+1}\left(6 + 6\xi_{0,j}h + 2\xi_{1,j}h^2\right) + 6\xi_{2,j}h^3 = 0, \end{aligned} \tag{10}$$

where h is the step size. In the solution domain, Eq. (10) is used to evaluate nodal values between 1 and $J-1$ inclusive. Since the values of the nodal points at $j = 0$ and $j = J$ are known, the value of the imaginary node at $j = -1$ can be determined from the estimated water surface slope, S_{H}, at the inflow section. Using a similar discretization equation, Eq. (9), for the water surface slope at inflow section and the expanded form of Eq. (10) at $j = 0$, the explicit expression for the nodal value at $j = -1$ in terms of values of the nodal point 0 and 1 is

$$H_{-1} = \left(\frac{-1}{\Omega + 6\Pi}\right)\begin{pmatrix} H_1\chi + H_0\Psi \\ \quad + \Pi\left(6hS_{\mathrm{H}} - 3H_0 - 2H_1\right) \\ \quad + 6h^3\xi_{2,0} \end{pmatrix}, \tag{11}$$

where:

$$\Pi = -6 + \xi_{1,0}h^2; \quad \Psi = -18 - 12\xi_{0,0}h + 3\xi_{1,0}h^2;$$

$$\Omega = 18 + 6\xi_{0,0}h - 6\xi_{1,0}h^2; \quad \chi = 6 + 6\xi_{0,0}h + 2\xi_{1,0}h^2.$$

Equations (10) and (11) constitute the one-dimensional finite difference equivalent equations for the numerical model.

The solution of the nonlinear flow equation based on the two-point boundary value technique requires an initial estimate of the position of the free surface profile. Generally, such problems must be solved by iterative methods, which proceed from an assumed initial free surface position. For the iterative procedure, the required computational effort is dependent on the choice of the initial flow surface profile. In this work, the Bernoulli and continuity equations are employed to obtain the initial flow surface profile estimate. Then, to simulate the flow surface profile, Eq. (10) is applied at different nodal points within the solution domain and results in a banded system of nonlinear algebraic equations. These equations together with Eq. (11), and the two boundary values at the inflow and outflow sections, are solved by the Newton–Raphson iterative method with a numerical Jacobian matrix. The convergence of the solution is assessed using the following criterion:

$$\left(\sum_{j=1}^{m}\left|\delta H_j\right| \Big/ \sum_{j=1}^{m} H_j\right) \leq \text{tolerance},$$

where δH_j is the correction depth to the solution of the nodal point j at any stage in the iteration; m is the total number of nodes in the solution domain excluding nodes having known values. In this study, a tolerance of 10^{-6} is used for the convergence of the numerical solutions. This computational scheme is superior to the method employed by Fenton (1996) which was based on the specification of initial conditions only and showed instability due to parasitic solutions.

For the solution of the pressure equation, a finite difference approximation, Eq. (8), is inserted into Eq. (2) to discretize the derivative term in the equation. Since the nodal flow depth values are known from the solution of the flow profile equation, this discretized equation yields the bed pressure, P_{b} (for $z = Z_{\mathrm{b}}$, where Z_{b} is the channel bed elevation) at different nodal points.

6 Experimental set-up and procedure

The experimental investigation was carried out in a horizontal flume 7100 mm long, 380 mm deep, and 300 mm wide. The flume and the trapezoidal profile weirs were made of plexiglass. Water was supplied to the head tank from a sump through 115 mm diameter pipe with a valve for controlling the discharge. Various flow improving elements were provided upstream of the trapezoidal profile weirs to obtain a smooth flow without large-scale turbulence. Symmetrical trapezoidal profile weirs of 150 mm height, crest lengths 100, 150 and 400 mm, respectively, and side slope $1V : 2H$ were tested at different discharges. For the purpose of assessing the performance of the numerical model on rough boundary, the surface of the 150 mm weir model including the bed of the flume was roughened using pieces of mild steel wire screen with mesh size 6.5 mm square. The diameter of the wire from which the screen was made was 0.56 mm. This method of roughening has been used in the past for simulating bed roughness in free surface flow (see e.g. Bauer, 1954; Kindsvater, 1964). The roughened model was also tested at different discharges.

The velocity distributions of the flow at different sections were measured using an Acoustic Doppler Velocimeter (ADV) with a two-dimensional side-looking probe. A series of experiments were conducted before commencing the experimental work in the subcritical and supercritical flow regions to verify the accuracy of the velocity measurements using this instrument. The first-order uncertainty analysis method (Moffat, 1985; Coleman and Steele, 1995) was applied to determine the repeatability of the velocity measurements. Thirty measurements were taken at the selected two points ($z = 8.28$ and 133 mm) in the subcritical and one point ($z = 12$ mm) in the supercritical flow regions. At a 95% confidence level, the uncertainties in the mean velocity

measurements at $z = 8.28$, 133 and 12 mm were found to be ± 1.53, ± 0.96 and $\pm 0.61\%$, respectively.

A volumetric tank system was used to measure the discharge. The system consisted of a tank with plan dimensions of 200 cm by 150 cm and depth of 450 cm, and an inclined manometer (56.62° to the horizontal) for water level measurement in the tank. Tank filling time longer than 1 min was used to minimize errors associated with the starting and stopping of the stopwatch. The discharge measurement of this system was checked against predictions that were made based on the integration of the velocity profiles taken at two sections upstream of the weir model. The result indicated that the maximum error in the determination of the flow rate was 4%. It is important to note that the uncertainty related to the velocity measurements has some contribution to this error. The longitudinal flow surface profile was observed with a manual point gauge of reading accuracy 0.10 mm. For recording the bed pressure, steel pressure taps of external diameter 3 mm were fixed along the centreline of the weir model with maximum horizontal spacing of 80 mm, but the spacing was much closer near the edges of the weir crest. These pressure taps were connected to vertical water piezometers of reading accuracy 1 mm by long plastic tubes. For each experiment, the base reading for the pressure taps was obtained immediately after the flow was shut off. According to the criteria given by Ranga Raju *et al*. (1990), the effects of viscosity and surface tension on the experimental results were negligible.

7 Applications

The numerical model, developed in a previous section, was used for simulating steady flow over short- and broad-crested trapezoidal profile weirs for both subcritical and transcritical flow situations (on smooth and rough beds). In order to assess the effect of the streamline curvature on the solution of the models, free flow situations with different H_0/L_w values were considered (H_0 = total energy head over the weir crest, L_w = weir crest length). It is apparent that the magnitude of this ratio determines the degree of the curvature of the flow over the crest of the weir. For $H_0/L_w \leq 0.50$, the curvature of the streamline over the crest is insignificant except near the edges of the weir crest (see e.g. Bos, 1978). Consequently, the expected influence of the non-hydrostatic and/or non-uniform velocity distributions on the behaviour of the flow might be insignificant. Similarly for the subcritical flow situation, flow with different submergence ratios (the ratio of the downstream flow depth to the upstream depth of flow above the crest of the weir) was considered for the purpose of simulating submerged flow with different degrees of submergences. This ratio influences the nature of the submerged flow surface profile especially over the crest of the weir.

For all cases of flow simulations, the size of the steps was designed to be fine enough to meet the requirements of reasonable accuracy. All computational results presented here were independent of the effect of spatial step size.

8 Model results for smooth bed

As described before, this part of the experiment was performed in a laboratory flume made of plexiglass. For the simulation of flow over such boundary, a smooth boundary resistance law was applied for computing the friction slope.

8.1 Effect of Boussinesq coefficient values

Numerical simulation of transcritical flow over a short-crested weir with $H_0/L_w = 1.10$ was performed on different values of Boussinesq coefficient in order to examine the influence of the magnitude of this correction coefficient on the accuracy of the predictions. For this purpose numerically determined value of $\beta = 1.06$ from the observed velocity profile for $q = 691.6\,\text{cm}^2/\text{s}$ at heel of the weir and a maximum value of $\beta = 1.20$ for flow in a channel of complex cross-section (Chow, 1959) were used; assuming that these values are constant throughout the computational domain. Figure 2 illustrates the flow surface and bed pressure profiles predicted by the BTM model for different values of β. In this figure the non-dimensional flow surface elevation and bed pressure at any section, z/H_w and $P_b/(H_0 + H_w)$ (H_w = weir height), respectively, are shown versus the normalized distance from the axis of symmetry of the weir, x/H_w. As can be seen from this figure, the solutions of the model are not strongly influenced by the Boussinesq coefficient values. This indicates that assumption of β equal to unity to simplify the computational procedure in the present model does not cause any significant discrepancies between the predictions and the experimental data.

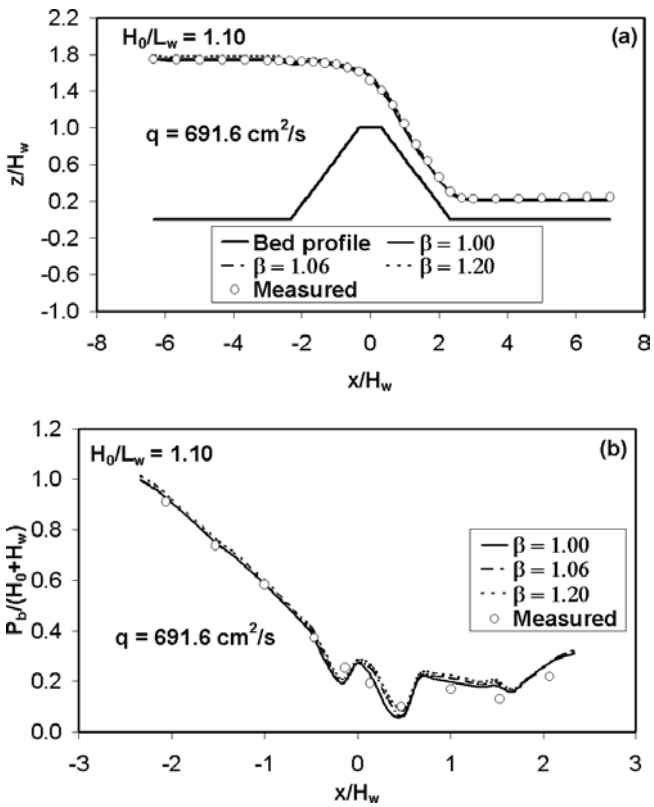

Figure 2 Comparison of predictions for various Boussinesq coefficient values ($L_w = 100$ mm).

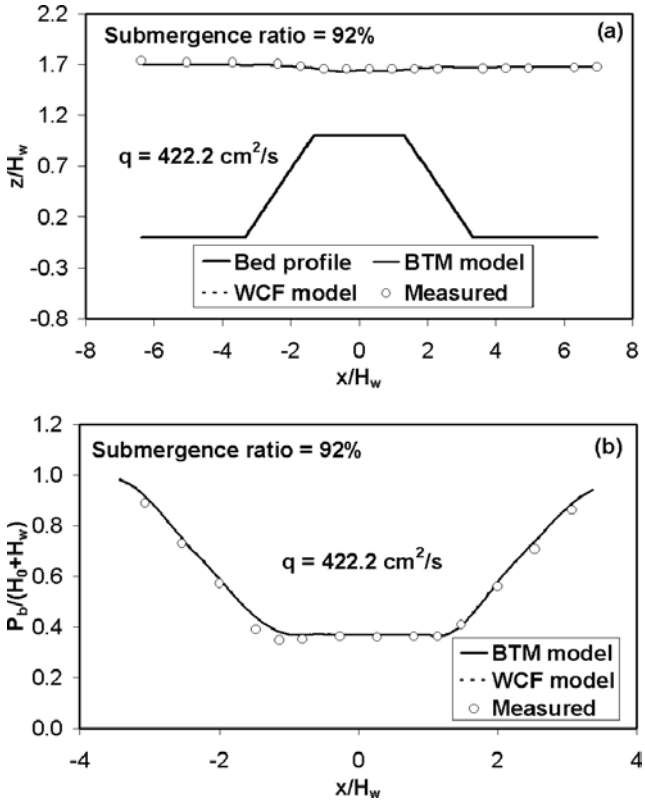

Figure 3 Submerged flow over a broad-crested weir: (a) flow surface profile; (b) bed pressure.

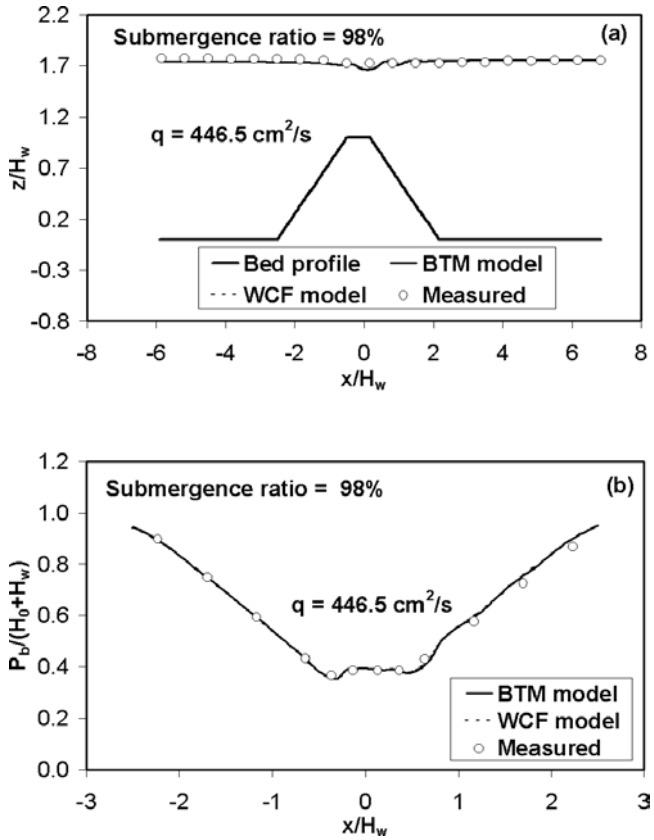

Figure 4 Submerged flow over a short-crested weir: (a) flow surface profile; (b) bed pressure.

8.2 Subcritical flow

The flow surface and bed pressure computation results of the numerical models are shown in Figs 3 and 4 for flow with submergence ratios of 92 and 98%. In this case the flow is nearly horizontal, the effects of non-hydrostatic pressure and non-uniform velocity distributions are expected to be insignificant. The modelled bed pressure and flow surface profiles using the BTM and WCF equations compare well with the measured data. Both equations overestimate the bed pressure near the upstream edge of the weir crest, with maximum absolute errors being less than 7.5% (see Fig. 3b). This discrepancy is attributed to burrs at the edges of the holes which may distort the pressure measurements. The flow surface profile solution of both models for the short-crested weir shows a train of standing waves over the crest of the weir, with mean absolute errors in the simulated profiles of only 1.4%. The predicted bed pressure for this part of the solution domain also reflects the simulated undular shape of the flow profile.

8.3 Transcritical flow

The computed flow surface and bed pressure profiles obtained for the case of transcritical flows over short- and broad-crested trapezoidal profile weirs are compared with experimental results in Figs 5–7. The numerical solutions of the BTM and WCF models for flow surface profile show excellent agreement with the measured data for both flow situations, the maximum absolute errors being only 1% for both models (see Figs 5a, 6a and 7a).

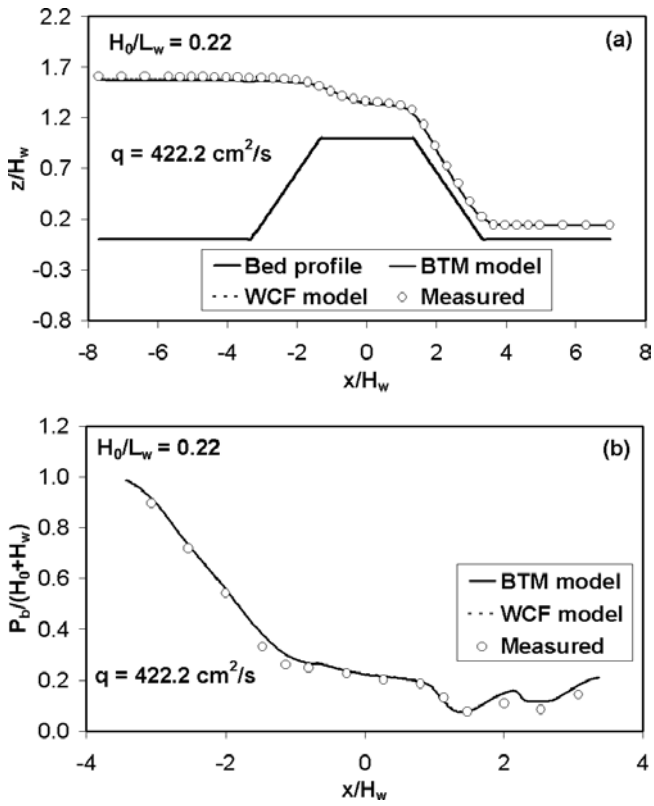

Figure 5 Flow surface and bed pressure profiles for flow over a broad-crested weir.

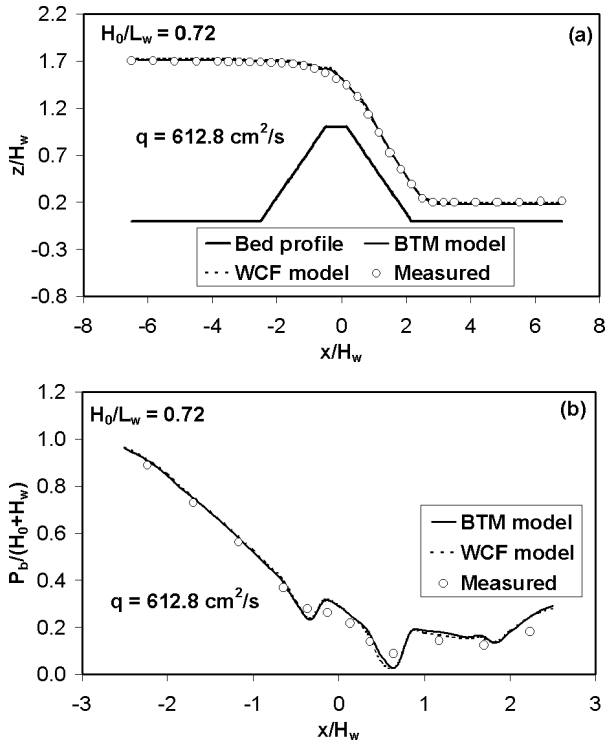

Figure 6 Flow surface and bed pressure profiles for flow over a short-crested weir ($L_w = 150$ mm).

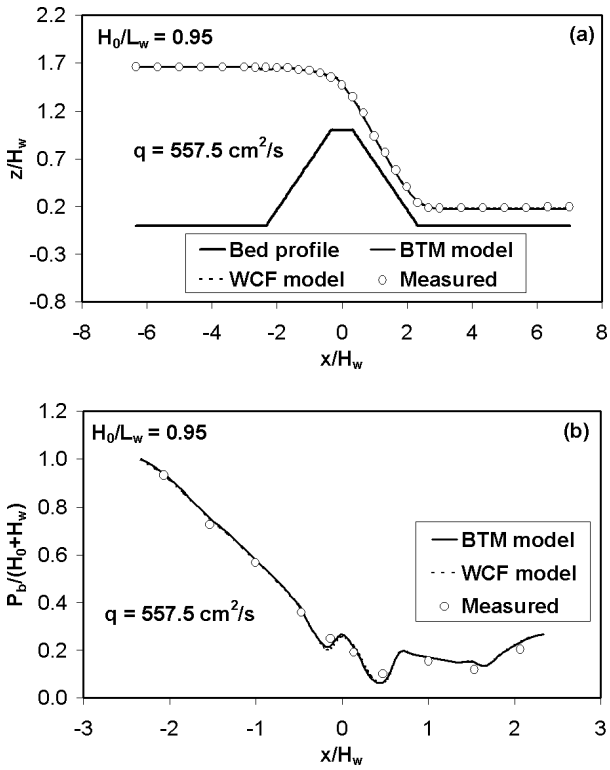

Figure 7 Flow surface and bed pressure profiles for flow over a short-crested weir ($L_w = 100$ mm).

The agreement particularly for flow with $H_0/L_w = 0.95$ is irrespective of the approximation of the curvature by the weakly curved flow expression. However, a small wobble is noticeable over the crest of the weir in the predicted flow surface profile for $H_0/L_w = 0.72$. A minor discrepancy between the predicted and measured values of the bed pressure is observed in the supercritical flow region on the downstream face of the weir. In this region the observed bed pressure might have some systematic errors due to turbulence effects. In general, the overall qualities of the numerical solutions of the bed pressure are good and show a satisfactory agreement with the experimental data (mean absolute errors = 5.6 and 6% for the BTM and WCF models, respectively). It is clear from Figs 6 and 7 that the pressure distribution on the crest of the weir is definitely non-hydrostatic due to the pronounced curvature of the streamlines ($H_0/L_w = 0.72$ and 0.95). The comparison result from these figures reveals that the WCF equation simulates the flow surface profile as accurately as the BTM equation with steep flow surface slope on the crest. This implies that the simplifying assumption of weak curvature of streamlines does not influence its numerical solutions at least for the flow problems considered. Also, this numerical experiment suggests that both models simulate the weir flow problem accurately regardless of the degree of curvature of the streamlines.

9 Model results for rough bed

9.1 Roughness parameters

For flow over rough boundaries, it is difficult to obtain a precise definition of the distance of the virtual bottom of the channel from the surface of the roughness for flow depth measurement. Different approaches have been introduced for locating the virtual bottom approximately. A simple and more popular method which utilizes the velocity distribution at a section was employed in this investigation. Accordingly, the plot of $u(z)$ versus $\log(z)$ was extrapolated in the region where the experimental velocity data follow the logarithmic law of velocity distribution. It was found that the virtual bottom was located at a distance of 0.28 mm below the surface of the wire screen.

The simulation of flow over a rough boundary also requires a predetermined value of roughness constant for computing the friction slope which is included in the equations. Assuming that the effects of roughness on the flow are purely frictional roughness, the Nikuradse equivalent sand roughness height, k_s, can be expressed as follows (Schlichting, 1960):

$$k_s = k \exp(3.4 - 0.40\,C), \tag{12}$$

in which k is the roughness height and C is a constant for the logarithmic velocity profile equation and equal to $u(z)/U_S - 5.75 \log(z/k)$, $u(z)$ is flow velocity at z and U_S is the shear velocity.

From the measured velocity profile at the upstream section, the constant C was estimated. Then, the equivalent roughness height was computed using Eq. (12). The Manning's roughness coefficient for the simulated bed was predicted based on the estimated k_s value of 1.864 mm and was taken as constant throughout the whole computational domain.

9.2 Subcritical flow

Figure 8 compares the predicted and observed values of the flow and bed pressure profiles for flow with submergence ratio

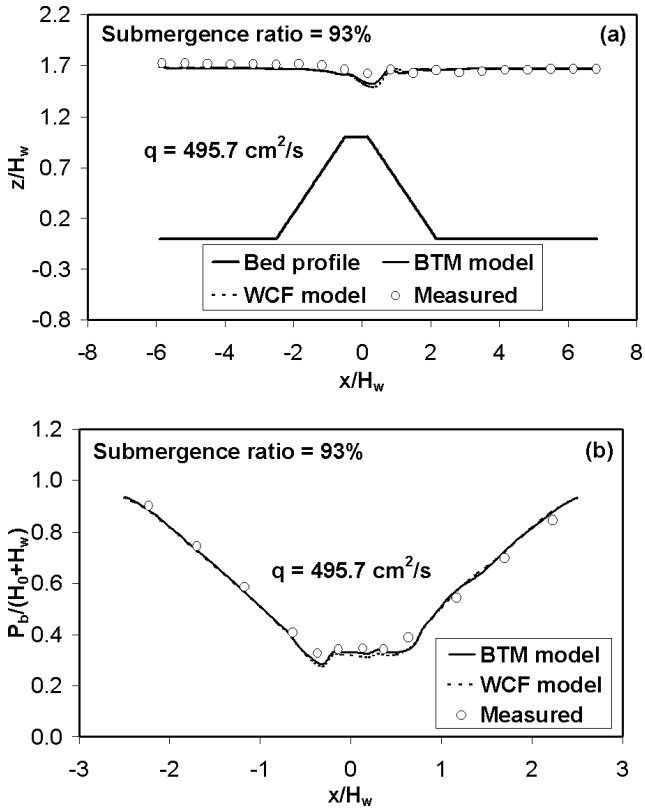

Figure 8 Flow surface and bed pressure profiles for submerged flow over a rough bed weir.

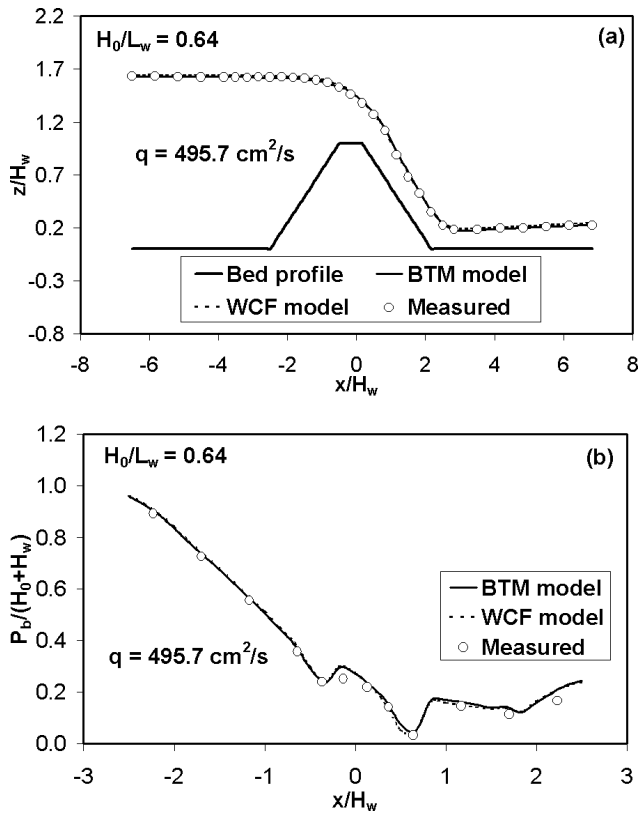

Figure 9 Flow surface and bed pressure profiles for transcritical flow over a rough bed weir.

93%. The results of the models for flow profile show excellent agreement with experimental data except at the crest where both models underestimate the flow depths. The maximum differences between the experimental data and the corresponding numerically simulated values around the crest of the weir for the BTM and WCF models are only 1.9 and 3.7%, respectively. It can be seen from Fig. 8(b) that the agreement of the predicted bed pressure with experimental data is good for the upstream and downstream faces of the weir. However, the WCF model underpredicts the bed pressure (maximum absolute error = 7.1%) at the crest of the structure. The overall level of agreement for the bed pressure is marginally better with the BTM model, the maximum absolute error being only 4.5%. Since the WCF model is a weak curvature approximation to the BTM model, minor difference between the overall performances of these two models is observed for this flow situation.

9.3 Transcritical flow

The computed and measured flow surface and bed pressure profiles are shown in Fig. 9. Upstream of the toe of the weir, the flow profile results of the two models agree well with the experimental data. In the supercritical flow region downstream of the toe of the weir, the WCF model predicts a slightly higher water surface elevation, with a mean absolute error of only 2%. Both models give almost similar bed pressure prediction for the entire flow region and the results are in good agreement with measurement.

The simulation results for flow over smooth and rough beds show that the BTM model predicts accurately the upstream flow surface elevation and flow transition from sub- to super-critical state irrespective of the curvature of the streamline of the flow. This suggests that this model can be employed to develop head–discharge relationships for trapezoidal profile weirs under free flow conditions.

10 Summary and conclusions

Two one-dimensional Boussinesq-type momentum equation models were investigated for modelling free surface flow problems with weak and strong curvature of streamlines in both frictionless and frictional channels. One model, the BTM equation incorporates relatively a higher degree of approximation for the effect of non-hydrostatic pressure distribution, and the other, the WCF equation model is the simplified version of this model for flow situations that involve weak streamline curvature and slope. Free and submerged flows over broad- and short-crested trapezoidal profile weirs with smooth and rough flow boundaries were considered for simulation purpose. Finite difference approximations were used to discretize the flow equations. The resulting nonlinear algebraic equations were solved using the Newton–Raphson technique with a numerical Jacobian matrix. Comparison of the numerical prediction results with experimental data was also presented. A good agreement was obtained between the simulated and measured data.

For submerged flow over a short-crested trapezoidal profile weir, both models satisfactorily predicted the shape of the flow profiles over the crest of the weir. The crest bed pressure

prediction of the BTM model showed a slightly better agreement (maximum absolute error = 4.5%) with measurement than the WCF model for flow with submergence ratio of 93%, but both models provided similar and accurate predictions for the bed pressure on the upstream and downstream faces of the weir. Generally speaking, the overall performance of both models for subcritical flow over short- and broad-crested weirs was reasonably good.

The result presented in this paper underline the satisfactory performance of the WCF model in predicting transcritical flows with strong streamline curvatures. This is surprising considering that the WCF model has not been developed to treat such flows.

Acknowledgments

The experimental work presented in this paper was done in the Michell Laboratory of the University of Melbourne, Australia. The writers are thankful to Mr. Joska Shepherd and Mr. Geoffrey Duke for building the experimental arrangement. The writers appreciate the valuable comments from the reviewers.

Notation

BTM = Boussinesq-type momentum
C = Constant for logarithmic velocity distribution
Fr = Froude number
g = Acceleration due to gravity
h = Step size in the horizontal direction
H = Depth of flow measured vertically from the bed
H_0 = Total energy head over the crest of the weir
H_w = Height of the weir
k = Roughness height
k_s = Nikuradse equivalent sand roughness height
L_w = Crest length of the weir
m = Total number of nodal points in the solution domain
p = Pressure
P_b = Bed pressure
q = Discharge per unit width of the channel
S_f = Friction slope
S_H = Slope of the flow surface
S_0 = Slope of the bed
$u(z)$ = Horizontal flow velocity at z
U_S = Shear velocity
WCF = Weakly curved flow
x = Horizontal coordinate
y = Transverse coordinate
z = Vertical coordinate
Z_b = Channel bed elevation
Z_b', Z_b'', Z_b''' = Derivatives of the bed profile
β = Boussinesq coefficient
δH_j = Correction depth at node j
η = Mean elevation of the free surface
θ = Angle of inclination of the streamline with the horizontal
κ = Curvature of a streamline
κ_b = Curvature of the bed
κ_H = Curvature of the flow surface
ξ = Nonlinear term associated with the flow equation
ρ = Density of the fluid
ω_0 = Weighting factor

References

1. ABBOTT, M.B. (1979). *Computational Hydraulics; Elements of the Theory of Free Surface Flow*. Pitman Publishing Limited, London, UK.
2. BAUER, W.J. (1954). "Turbulent Boundary Layer on Steep Slopes". *Trans. ASCE* 119, 1212–1233.
3. BHALLAMUDI, S.M. and CHAUDHRY, M.H. (1992). "Computation of Flows in Open Channel Transitions". *J. Hydraul. Res.* 30(1), 77–93.
4. BERGER, R.C. (1994). "Strengths and Weaknesses of Shallow Water Equations in Steep Open Channel Flow". *Hydraul. Engng. Proc. Nat. Conf. ASCE* 2, 1257–1262.
5. BICKLEY, W.G. (1941). "Formulae for Numerical Differentiation". *Math. Gaz.* 25, 19–27.
6. BOS, M.G. (1978). *Discharge Measurement Structures*. International Institute for Land Reclamation and Improvement, Wageningen, The Netherlands.
7. BOUSSINESQ, J. (1877). Essai sur la théorie des eaux courantes. *Mémories présentés par divers savants à l'Académie des Sciences* (*Paris*) 23, 1–680.
8. CHOW, V.T. (1959). *Open Channel Hydraulics*. McGraw-Hill Book Co., New York, NY.
9. COLEMAN, H.W. and STEELE, W.G. (1995). "Engineering Application of Experimental Uncertainty Analysis". *AIAA J.* 33(10), 1888–1896.
10. DRESSLER, R.F. (1978). "New Nonlinear Shallow Flow Equations with Curvature". *J. Hydraul. Res.* 16(3), 205–220.
11. FENTON, J.D. (1996). "Channel Flow Over Curved Boundaries and a New Hydraulic Theory". *Proceedings of the* 10*th Congress of APD-IAHR*, Langkawi, Malaysia, Vol. 2, pp. 266–273.
12. FRITZ, H.M. and HAGER, H.W. (1998). "Hydraulics of Embankment Weirs". *J. Hydraul. Engng. ASCE* 124(9), 963–971.
13. HAGER, W.H. and HUTTER, K. (1984). "Approximate Treatment of Plane Channel Flow". *Acta Mech.* 51, 31–48.
14. HAGER, W.H. (1985). "Equation of Plane, Moderately Curved Open Channel Flows". *J. Hydraul. Engng. ASCE* 111(3), 541–546.

15. KHAN, A.A. and STEFFLER, P.M. (1996a). "Vertically Averaged and Moment Equations Model for Flow Over Curved Beds". *J. Hydraul. Engng. ASCE* 122(1), 3–9.
16. KHAN, A.A. and STEFFLER, P.M. (1996b). "Modelling Overfalls Using Vertically Averaged and Moment Equations". *J. Hydrual. Engng. ASCE* 122(7), 397–402.
17. KINDSVATER, C.E. (1964). *Discharge Characteristics of Embankment Shaped Weirs*. Geological Survey Water Supply Paper 1617-A, U.S., Government Printing Office, Washington, DC.
18. MATTHEW, G.D. (1991). "Higher Order, One-dimensional Equations of Potential Flow in Open Channels". *Proceedings of the Institution of Civil Engineers*, London, England, Vol. 91, pp. 187–201.
19. MOFFAT, R.J. (1985). "Using Uncertainty Analysis in the Planning of an Experiment". *J. Fluids Engng. ASME* 107, 173–178.
20. RANGA RAJU, K.G., SRIVASTAVA, R. and POREY, P.D. (1990). "Scale Effects in Modelling Flows Over Broad-crested Weirs". *J. Irrig. Power* 47(30), 101–106.
21. SCHLICHTING, H. (1960). *Boundary Layer Theory*. McGraw-Hill Book Company, New York.
22. SIVAKUMARAN, N.S., HOSKING, R.J. and TINGSANCHALI T. (1983). "Steady Shallow Flow Over Curved Beds". *J. Fluid Mech*. 128, 469–487.
23. SIVAKUMARAN, N.S. and YEVJEVICH, V. (1987). "Experimental Verification of the Dressler Curved-flow Equations". *J. Hydraul. Res.* 25(3), 373–387.
24. STEFFLER, P.M. and JIN, Y. (1993). "Depth Averaged and Moment Equations for Moderately Shallow Free Surface Flow". *J. Hydraul. Res*. 31(1), 5–17.